

Exciton-light coupling in (In,Ga)As/GaAs quantum wells in a longitudinal magnetic field

P. S. Grigoryev and I. V. Ignatiev

Spin Optics Laboratory, St. Petersburg State University, Ulyanovskaya 1, Petrodvorets, 198504 St. Petersburg, Russia

V. G. Davydov, Yu. P. Efimov, S. A. Eliseev, V. A. Lovtcius, and P. Yu. Shapochkin

Department of Physics, St. Petersburg State University, Ulyanovskaya 1, Petrodvorets, 198504 St. Petersburg, Russia

M. Bayer

*Experimentelle Physik 2, Technische Universität Dortmund, D-44221 Dortmund, Germany
and Ioffe Physical-Technical Institute, Russian Academy of Sciences, 194021 St. Petersburg, Russia
(Received 30 June 2017; revised manuscript received 21 September 2017; published 3 October 2017)*

We report on the observation of a significant increase of the radiative decay rates for exciton transitions in a wide (In,Ga)As/GaAs quantum well ($L = 95$ nm) in magnetic fields up to 6 T applied along the growth axis of the heterostructure. The absolute values of the radiative decay rates are obtained from a quantitative analysis of resonant features in the experimentally measured reflectance spectra in the range of the optical transitions to the quantum-confined exciton states. High crystalline quality of the heterostructure allows us to observe the ground and several excited exciton transitions with the nonradiative broadening comparable to the radiative one. We employ a numerical procedure appropriate for the studied wide quantum well to model the increase of the radiative decay rate in magnetic field. The results of the modeling agree well with the experimental data.

DOI: [10.1103/PhysRevB.96.155404](https://doi.org/10.1103/PhysRevB.96.155404)**I. INTRODUCTION**

An external magnetic field may induce several interesting effects for excitons in semiconductor heterostructures. Thanks to the very controllable action of magnetic field on a quantum system, it is widely used for observation of interesting phenomena as for quantitative characterization of excitons in heterostructures. The magnetic field causes a diamagnetic shift and a Zeeman splitting of exciton states, which have been widely studied for bulk crystals [1,2] and single quantum wells (QWs) [3–6]. Coupling of excitons with light in a QW embedded in a microcavity is found to be very sensitive to the application of magnetic field [7–13]. Many works have been devoted to indirect excitons in double-QW structures in magnetic field, whose long lifetime allows one to study, in particular, their dipole-dipole interaction [14,15] and transport across the magnetic field [16–18]. The spin dynamics of excitons and charged carriers is another research area where the magnetic field plays a crucial role [19–25]. Recently, various interesting phenomena could be revealed for Rydberg excitons in bulk Cu_2O crystals subject to a magnetic field and studied thanks to the development of a high-precision experimental technique and careful theoretical modeling [26,27].

The magnetic-field-induced modification of the exciton-light coupling is another effect, widely studied for bulk crystals [1,2] and for QW heterostructures [12,17,28–34]. Usually an increase of the intensities of spectral features is observed in absorption or reflectance spectra. In bulk crystals, the application of magnetic field induces the appearance of multiple resonant peculiarities, which originate from the $1s$ - $2s$ -, etc., exciton states [2]. Their energy positions as functions of the magnetic field form the so-called fan diagram, which can be understood in terms of optical transitions between electron and hole Landau levels with a correction from the electron-hole Coulomb interaction. The intensity of the features is experimentally found to increase with magnetic field. A theoretical analysis is considerably hampered because

of the overlap of the Landau states with the continuous spectrum of states in bulk [2].

The spectral peculiarities in QWs are related to the quantum confined $1s$ -like exciton states. In earlier works [28–32], the lowest quantum-confined states in relatively narrow QWs were experimentally studied. The moderate quality of samples did not allow one to obtain precise data about the exciton-light coupling. Correspondingly, their theoretical analysis was rather qualitative than quantitative.

The exciton-light coupling is usually discussed in terms of quantities such as the exciton oscillator strength, the longitudinal-transverse splitting, the radiative recombination (or decay) rate, Γ_0 , or the radiative broadening, $\hbar\Gamma_0$. These quantities are related to each other via the fundamental constants and material parameters. The definitions of first two terms can be found in the textbook by Ivchenko [1], for example. We use in the present work the latter terms, whose definitions are given below. The physical origin of the magnetic-field-induced increase of the radiative recombination rate is well established [1]. The magnetic field considerably modifies the internal electron-hole motion in the exciton when the magnetic length λ_B becomes comparable to or smaller than the Bohr radius of the exciton a_B . In the case of GaAs, the critical magnetic field, when $\beta = a_B/\lambda_B \sim 1$, is about 4 T. In strong magnetic field, $\beta > 1$ (the Elliott-Loudon criterion [35]), the overlap of the electron and hole wave functions becomes stronger than that caused solely by their Coulomb attraction in the exciton. Correspondingly, the probability for the electron and the hole to be in the same unit cell and to recombine increases resulting in the increase of the exciton-light coupling.

Although this picture is transparent, the quantitative analysis of the exciton-light coupling requires both the careful experimental study of a high-quality heterostructure and the rather complex numerical calculation of the exciton wave functions in an external magnetic field. GaAs-based high-quality structures have become available in the last two decades

due to the development and refinement of the technology of molecular beam epitaxy (MBE). The theoretical analysis, on the other hand, requires the solution of the three-dimensional Schrödinger equation for an exciton in a quantum well in a longitudinal magnetic field applied along the heterostructure growth axis (the Faraday geometry). Several approximate methods have been developed for solution of this problem [17,36–40]. They are applied mainly to excitons in narrow QWs where these methods can be asymptotically exact. Recently, a method of an exact numerical solution of the equation applicable for the exciton problem in QWs of arbitrary width and potential profile has been proposed [34].

In this work, we study the exciton-light coupling in a heterostructure with a wide (In,Ga)As/GaAs QW subject to a magnetic field applied along the growth axis. The superior quality of the structure allows us to observe several quantum-confined exciton states as a set of narrow resonances in the reflectance spectra. The strong energy shift, state splitting, and increase of intensity of the resonances are observed in the magnetic field. We theoretically model the resonances and their modification in the magnetic field by the exact numerical solution of the respective Schrödinger equation. The comparison of the experimentally obtained and theoretically calculated constants of the exciton-light coupling as a function of the magnetic field shows good agreement without any fitting parameters.

II. EXPERIMENT

The heterostructure under study was grown by MBE technology. It contains an (In,Ga)As/GaAs QW of nominal width $L = 95$ nm with an indium content of about 2%. Besides the QW, the heterostructure contains several layers for improving material quality and also a narrow QW, which are out of the scope of the present study. The high quality of the heterostructure was verified by photoluminescence and reflectance spectroscopy of the exciton resonances corresponding to the optical transitions from or to the quantum-confined exciton states in the wide QW. In particular, the nonradiative broadening of resonances was found to be several tens of μeV only, which is comparable to the radiative broadening of the resonance corresponding to the ground exciton transition. Further details of the optical characterization of the heterostructure can be found in Refs. [5,41].

The sample was cooled down to $T \approx 15$ K in a closed-cycle cryostat with a superconductive magnet allowing for application of magnetic fields up to 6 T. The sample temperature was optimized to suppress the excess nonradiative broadening of exciton resonances caused by an accumulation of nonradiative excitons (see Ref. [41] for details). The magnetic field was applied along the growth axis of the heterostructure.

We measured reflectance spectra in the spectral range of several low-lying exciton transitions in the wide QW. An incandescent lamp was used as light source for the measurements. The radiation of the lamp was passed through a $50\text{-}\mu\text{m}$ pinhole and a color filter cutting off the visible range of the spectrum, and then focused onto the sample close to normal incidence. The excitation power was about 10 mW/cm^2 across the spectrum. The reflected light beam was directed into a 0.5-m spectrometer and detected by a cooled

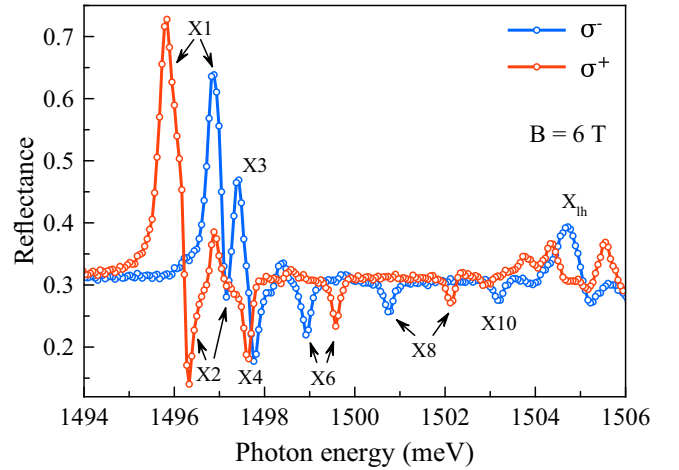


FIG. 1. Reflectance spectra of the 95-nm wide $\text{In}_{0.02}\text{Ga}_{0.98}\text{As/GaAs}$ QW measured in the σ^+ (red curve) and σ^- (blue curve) polarizations at $B = 6$ T. The symbols “X1,” “X2” etc. mark the respective exciton resonances.

charge-coupled device. The spectra were measured for two circular polarizations selected by means of a $\lambda/4$ wave plate and a linear polarizer placed in front of the spectrometer.

Examples of reflectance spectra measured at a magnetic field of $B = 6$ T are shown in Fig. 1. The spectra show several narrow features (resonances) labeled as X1, . . . , X10. These resonances correspond to optical transitions to the quantum confined states of the heavy-hole exciton in the QW. The relatively broad resonances X_{lh} correspond to the light-hole exciton states, split off from the heavy-hole exciton states due to the mechanical strain in the heterostructure caused by the lattice constant mismatch between the GaAs and $\text{In}_{0.02}\text{Ga}_{0.98}\text{As}$ layers. Hereafter we will discuss the states of the heavy-hole exciton only.

The resonances that appear to be similar to each other in the spectra measured for opposite polarizations are shifted relative to each other, which points towards the Zeeman splitting of the involved exciton states. This splitting is extensively discussed in Ref. [5]. The splitting is relatively large for the state X1 and almost zero for the state X4. Due to the splitting, the energy separation between the states X1, X2, and X3 in the σ^- -polarized spectrum becomes smaller than their broadening and the amplitudes of these resonances can be determined only with large uncertainties. In particular, the resonance X2 disappears almost completely in the spectrum. We, therefore, consider exclusively the spectra measured in σ^+ polarization below.

Figure 2 shows a representative set of spectra measured at different magnetic fields. As seen, the application of the magnetic field results in a considerable shift of the exciton resonances to the higher energies which results from the well-known diamagnetic shift [1]. Another important effect of the magnetic field is a significant increase of the amplitudes of all resonances. This is a clear indication of the magnetic-field-induced increase of the exciton-light coupling.

To quantitatively assess the strength of the exciton-light interaction, we use the phenomenological model of the reflectance spectra described in Ref. [1] and generalized in

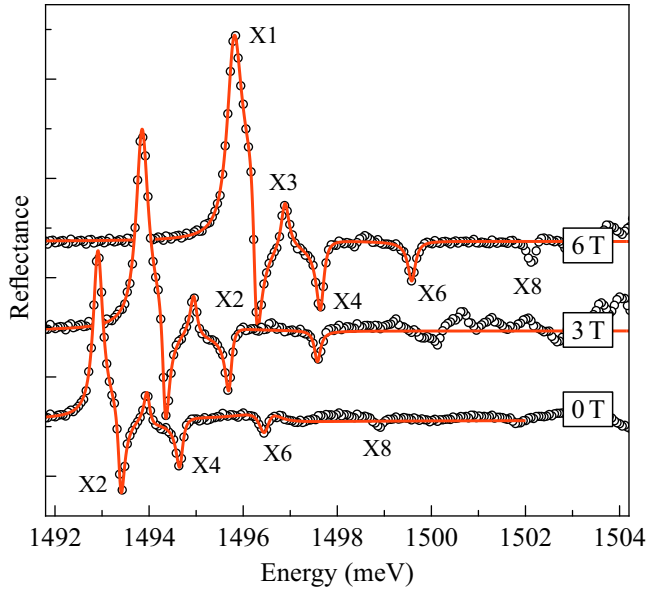


FIG. 2. Reflectance spectra of the 95-nm-wide InGaAs/GaAs QW in magnetic fields up to 6 T measured in the σ^+ circular polarization (symbols). The solid lines show fits by Eqs. (1) and (2). The spectra are shifted vertically for clarity.

Refs. [41,42] for the case of multiple exciton transitions. The model considers the reflection from the sample surface, described by the reflection amplitude r_s , and the resonant reflection from the QW, described by the amplitude coefficients r_j , for each exciton resonance j :

$$r_j = \frac{i\Gamma_{0j}}{\tilde{\omega}_{0j} - \omega - i(\Gamma_j + \Gamma_{0j})}. \quad (1)$$

Here the parameter Γ_{0j} describes the radiative decay rate of the j th exciton state, Γ_j is the rate of nonradiative relaxation from this state, and $\tilde{\omega}_{0j}$ is the frequency of the exciton transition j . These three quantities are considered to be fitting parameters of the model for each particular exciton resonance.

The total reflection from the heterostructure is then described by

$$R = \left| \frac{r_s + \sum_j r_j e^{i\phi_j}}{1 + r_s \sum_j r_j e^{i\phi_j}} \right|^2. \quad (2)$$

This expression contains one more set of fitting parameters ϕ_j , describing the phase shift of the light wave reflected from the QW relative to the wave reflected from the sample surface at the frequency of the corresponding exciton resonance. For the case of a symmetric QW potential, the phases of even and odd resonances differ by π : $\phi_{2j-1} = \phi_{2j} \pm \pi$ [42]. For the structure under study, the phase shift of the light wave propagating from the sample surface and back is about 2π . This is why the first exciton resonance (X1) appears as a peak, the second one as a dip, and so on (see Figs. 1 and 2).

The potential profile of the QW under study is slightly asymmetric because of segregation of indium during the MBE growth of the heterostructure [42]. This effect causes a deviation from the simple relation between the phases of

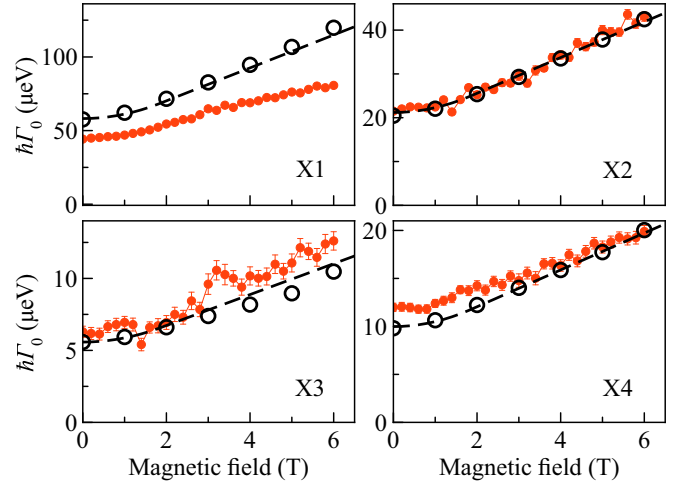


FIG. 3. Radiative broadening for the first four exciton states in the 95-nm QW as a function of magnetic field. The red circles are the values of $\hbar\Gamma_{0j}$ extracted from the experiment. The open circles are the numerically calculated radiative decay rates and the dashed lines are the fittings of these results according to Eq. (11).

even and odd resonances and we have to consider all the phases as fitting parameters. Although there are four fitting parameters for each resonance, the good spectral separation between the resonances allows one to reliably determine these parameters and to accurately fit the spectra by Eqs. (1) and (2). The associated fitting curves are shown in Fig. 2.

We determined the fitting parameters for each value of magnetic field and thereby obtained their dependencies on the magnetic field. The dependencies of the radiative broadening $\hbar\Gamma_{0j}$ for the four lowest resonances are shown in Fig. 3. As seen, the radiative broadening gradually increases with magnetic field for all the exciton resonances. The theoretical modeling of this effect is described in the next section.

The energies of the exciton resonances, $\hbar\tilde{\omega}_{0j}$, are found to depend quadratically on the magnetic field in the range 0–2 T and then tend to the expected linear dependency in larger magnetic fields. The energy shift of the resonances is related to the diamagnetic shift of the exciton states [1,6] as well as to their Zeeman splitting [5]. We do not discuss these effects in the present paper any further.

The fitting parameters Γ_j and ϕ_j should be less sensitive to the magnetic field. The experimental data processing shows that the nonradiative broadenings $\hbar\Gamma_j$ are almost independent of the magnetic field within the experimental error: $\hbar\Gamma_1 = 54 \pm 2 \mu\text{eV}$ (for $B = 0 \dots 4$ T), $\hbar\Gamma_2 = 73 \pm 4 \mu\text{eV}$, $\hbar\Gamma_3 = 73 \pm 10 \mu\text{eV}$, and $\hbar\Gamma_4 = 83 \pm 5 \mu\text{eV}$. The exception is the increase of $\hbar\Gamma_1$ from 54 to 65 μeV when the magnetic field increases from 4 to 6 T. The broadening increase is possibly caused by a suppression of the electron diffusion from the excited area of the sample [11].

The phase shift obtained in the fits are also almost insensitive to the magnetic field. Their average values are $\phi_1 = 0.01 \pm 0.05$, $\phi_2 = 2.93 \pm 0.08$, $\phi_3 = 0.31 \pm 0.012$, $\phi_4 = 3.52 \pm 0.08$. A small decrease of the phases of order of several percent is observed at large magnetic field strengths.

III. EXCITON-LIGHT COUPLING

The coupling of an exciton with a light wave can be characterized by the radiative decay rate Γ_0 , or the radiative lifetime $\tau = 1/(2\Gamma_0)$. A consistent theory of the coupling for an isolated exciton state with a light wave is described in Ref. [1]. It gives rise to the following expression for Γ_0 :

$$\Gamma_0 = \frac{2\pi q}{\hbar\epsilon} \left(\frac{e|p_{cv}|}{m_0\omega_0} \right)^2 \left| \int_{-\infty}^{\infty} \Phi(z) \exp(iqz) dz \right|^2. \quad (3)$$

Here m_0 is the free-electron mass, e is the electron charge, ω_0 is the exciton resonance frequency, $q = \sqrt{\epsilon}\omega_0/c$ is the light wave vector, ϵ is the average dielectric constant of the heterostructure, and $|p_{cv}|$ is the matrix element of the momentum operator between the Bloch states in the conduction and valence bands. The function $\Phi(z)$ is the one-dimensional cut of the envelope of the exciton wave function along the growth axis $\{x_e = x_h = 0, y_e = y_h = 0, z_e = z_h = z\}$.

Expression (3) was derived for relatively narrow QWs, for which the quantum-confined exciton states are well separated from each other. A more general theory considering the light-induced coupling of different exciton states in wide QWs was proposed in Ref. [43]. The analysis, however, shows that expression (3) is applicable if the radiative broadening $\hbar\Gamma_0$ is much smaller than the energy separation between the neighboring exciton states. This is the case for the structure we study. Therefore we use the simplified theory of Ref. [1] and, correspondingly, expression (3) for characterizing the exciton-light coupling.

To calculate Γ_{0j} , we have to solve the corresponding Schrödinger equation for an exciton in a QW subject to the longitudinal magnetic field and determine the exciton wave functions for several quantum-confined exciton states. The Hamiltonian of the problem for the s -like excitons is given by

$$H = E_g + T_e + T_h - \frac{e^2}{\epsilon r} + V(z_e, z_h) + \frac{1}{2\mu} \left(\frac{eB}{2c} \rho \right)^2. \quad (4)$$

Here E_g is the band gap, $T_e(T_h)$ is the conduction (valence)-band kinetic term. The fourth term describes the electron-hole Coulomb interaction with r being the relative electron-hole distance. The next term, $V(z_e, z_h)$, is the QW potential for electron and hole along the z axis. The last term corresponds to the parabolic potential in the QW layer created by the magnetic field. Here ρ is the electron-hole separation transverse to z axis. In expression (4) we have omitted the terms describing the Zeeman splitting of the exciton states as they do not affect the exciton-light coupling.

The conduction band in GaAs-based heterostructures is characterized by the effective electron mass, while the valence band consists of the heavy-hole (hh) and light-hole (lh) subbands and is described by the Luttinger Hamiltonian [44]. Generally the hole subbands are coupled, however, the quantum confinement in the QW splits the subbands, thus reducing the coupling. The coupling is further suppressed in our case by the strain-induced hh-lh splitting (see Fig. 1 and related discussion). Therefore the hh-lh coupling can be neglected in the calculations. In addition, the QW potential and the strain reduce the symmetry of the valence band, resulting

in anisotropic hole masses,

$$\begin{aligned} m_{hhz(lhz)} &= m_0/(\gamma_1 \mp 2\gamma_2), \\ m_{hhxy(lhxy)} &= m_0/(\gamma_1 \pm \gamma_2), \end{aligned} \quad (5)$$

where γ_1 and γ_2 are the Luttinger parameters and m_0 is the free-electron mass. In the calculations described below, we used for these parameters the values $\gamma_1 = 6.98$ and $\gamma_2 = 2.06$ for GaAs crystals, taken from Ref. [45].

Generally speaking, the magnetic field induces an additional hh-lh coupling resulting, in particular, in a renormalization of the exciton g factor [5]. Our estimates, however, show that this coupling leads to a small modification of the exciton wave functions only (less than 2%) which is insufficient for affecting notably the calculations of the radiative decay rates. We, therefore, neglect the coupling and consider the cylindrically symmetric eigenvalue problem:

$$\begin{aligned} & \left[-\frac{\hbar^2}{2\mu} \left(\frac{\partial^2}{\partial \rho^2} - \frac{1}{\rho} \frac{\partial}{\partial \rho} + \frac{1 - k_\varphi^2}{\rho^2} \right) + \frac{e\hbar B}{2c} \left(\frac{m_h - m_e}{M\mu} \right) k_\varphi \right. \\ & - \frac{\hbar^2}{2m_e} \frac{\partial^2}{\partial z_e^2} - \frac{\hbar^2}{2m_h} \frac{\partial^2}{\partial z_h^2} - \frac{e^2}{\epsilon \sqrt{\rho^2 + (z_e - z_h)^2}} + V(z_e, z_h) \\ & \left. + \frac{1}{2\mu} \left(\frac{eB}{2c} \rho \right)^2 \right] \chi(z_e, z_h, \rho) = E \chi(z_e, z_h, \rho). \end{aligned} \quad (6)$$

Here $\mu = (1/m_e + 1/m_{hxy})^{-1}$ is the reduced exciton mass with m_{hxy} as hole mass. This Hamiltonian is similar to the diagonal part of the Hamiltonian used in Ref. [5] without the terms describing the interaction of the hole and electron angular momenta with the magnetic field.

The function $\chi(z_e, z_h, \rho)$ is related to the exciton wave function as

$$\psi(X, Y, \rho, \varphi, z_e, z_h) = \psi_{CM}(X, Y) \frac{\chi(z_e, z_h, \rho)}{\rho} e^{ik_\varphi \varphi}. \quad (7)$$

ψ_{CM} is the product of plane waves along the X and Y directions describing the exciton center-of-mass motion in the QW plane. For the experimental conditions considered here, the in-plane components of the exciton wave vector are zero and ψ_{CM} is a properly normalized constant. The exponential function in Eq. (7) describes the exciton states with different projections k_φ of the orbital angular momenta on the z axis. In linear optical spectroscopy, the optically active exciton states are the s -like states with $k_\varphi = 0$ and this function is equal to unity. The denominator ρ in Eq. (7) is introduced to apply a zero boundary condition for $\chi(z_e, z_h, \rho)$ at $\rho = 0$ [34].

The three-dimensional eigenproblem (6) can be solved numerically using the algorithm described in Ref. [34]. To illustrate the general behavior of the radiative decay rates of the exciton states in magnetic field, we calculated the exciton wave functions for rectangular (In,Ga)As QWs of different widths. The finite-difference method was applied on a rectangular mesh with at least $70 \times 70 \times 200$ points along the z_e , z_h , and ρ directions in a volume ranging from $40 \times 40 \times 400$ nm³ for narrow QWs to $200 \times 200 \times 400$ nm³ for the widest QW. We considered QWs of width $L \leq 150$ nm where Eq. (3) is still applicable. The results of these calculations are shown in Fig. 4.

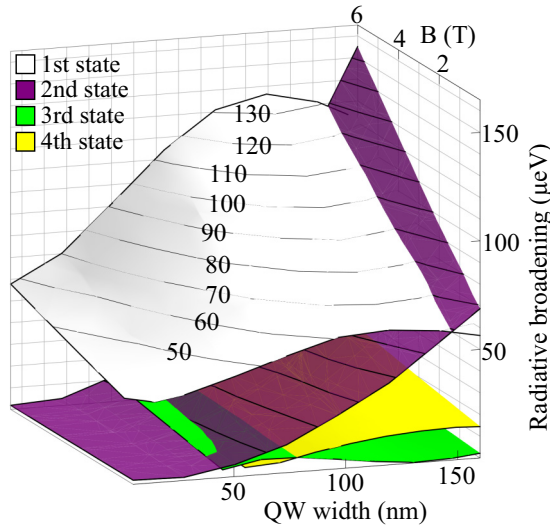


FIG. 4. Radiative decay rate as a function of the QW width and of the magnetic field for the first four quantum-confined exciton states in $\text{In}_{0.02}\text{Ga}_{0.98}\text{As}/\text{GaAs}$ QWs.

The dependence of the radiative decay rate on the QW width is mainly determined by the overlap of $\Phi(z)$ with the light wave described by the integral in Eq. (3). Function $\Phi(z)$ is defined from the numerically obtained exciton wave function as

$$\Phi(z) = \lim_{\rho \rightarrow 0} \frac{\chi(z, z, \rho)}{\rho}. \quad (8)$$

The overlapping integral in Eq. (3) reaches a maximum for the ground state when the QW width is about half of the wavelength, $L \approx 115$ nm in the (In,Ga)As QWs. For the second state, this maximum is reached for a QW of 230 nm width. However, Eq. (3) is not applicable for such a wide QW because the energy separation between the ground and the first excited state is comparable to the radiative broadening. The radiative decay rate for the third state drops down to zero in a QW of approximately 130 nm width. The behavior of $\hbar\Gamma_0$ of the fourth state is similar to that of the first state although its magnitude is considerably smaller.

In the presence of an external magnetic field, the radiative decay rate considerably rises with magnetic field (see Fig. 4). In particular, $\hbar\Gamma_{0j}$ becomes approximately twice larger in a magnetic field of $B = 6$ T for excitons in wide enough QWs ($L \geq 50$ nm). A similar effect has been theoretically predicted in Ref. [12]. We find that $\hbar\Gamma_{0j}$ demonstrates similar dependencies on the magnetic field for all the exciton states. They quadratically rise at relatively small magnetic fields with a transition to a linear dependence as the magnetic field increases. This linear dependence is a characteristic property of the diamagnetic exciton [2].

To analyze the exciton behavior in the heterostructure under study, we take into account the real potential profile of the QW. The profile $V(z_e, z_h)$ entering into Eq. (4) deviates from a rectangular shape due to segregation of In atoms during the growth process as extensively discussed in Ref. [42]. It has the form

$$V(z_e, z_h) = -f(z_e)V_c - f(z_h)V_v, \quad (9)$$

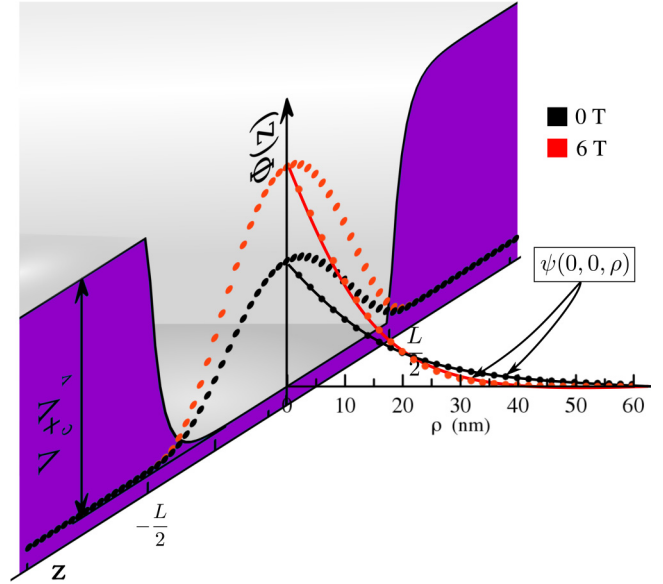


FIG. 5. Squeezing of the exciton wave function $\psi(z_e, z_h, \rho)$ in magnetic field for the heterostructure under study. Cross sections of the wave function along the direction $z_e = z_h = z$ at fixed $\rho = 0$ and along the direction ρ at fixed $z_e = z_h = 0$ are shown for zero magnetic field (black dots) and for $B = 6$ T (red dots). The purple area shows the QW potential profile for excitons along the growth axis.

where V_c and V_v are the maximum depth of the potential well in the conduction and valence bands, respectively. The function $f(z)$ is defined by the equations

$$\begin{aligned} f(z) &= (1 - e^{-z/\lambda_D}), & 0 < z < L, \\ f(z) &= (1 - e^{-L/\lambda_D})e^{-(z-L)/\lambda_D}, & z > L. \end{aligned} \quad (10)$$

Here $\lambda_D = 4.5$ nm is the segregation length (see Ref. [42]) and $L = 95$ nm is the nominal QW width. In the calculations, we used a ratio, $V_c : V_v = 2 : 1$, typical for GaAs-based heterostructures, and a total QW depth, $V_c + V_v = 23$ meV as follows from the experimental data (see Fig. 2). The bottom part of the modelled potential profile for excitons is shown in Fig. 5. As seen there, the In segregation notably smooths the potential profile at the GaAs/(In,Ga)As interface.

The effect of the magnetic field on the wave function $\psi(z_e, z_h, \rho) = \chi(z_e, z_h, \rho)/\rho$ of the lowest quantum-confined exciton state in the heterostructure under study is shown in Fig. 5. At zero magnetic field, the wave function has a cosinelike profile along the growth axis for $z_e = z_h = z$ and fixed $\rho = 0$. It decays exponentially along the ρ direction (see Fig. 5). When the magnetic field is applied, the cosinelike profile along the growth axis is preserved but the amplitude of wave function increases. The wave function decay along the ρ direction becomes faster and strongly nonexponential which hints at the magnetic-field-induced squeezing of the wave function that is extensively discussed in literature [1,2].

The exciton wave functions obtained by the numerical solution of Eq. (6) using the potential (9) allow us to calculate the radiative decay rate by the use of Eq. (3). The corresponding radiative broadenings $\hbar\Gamma_{0j}$ as functions of magnetic field are shown in Fig. 3. No fitting parameters were used for the calculations. As seen in the figure, there is a good

overall correspondence between the experimentally obtained and theoretically calculated magnetic-field dependencies of $\hbar\Gamma_{0j}$ for all the exciton transitions except for the first one. The possible origin of this discrepancy is discussed in the next section.

IV. DISCUSSION

The comparison of the experimentally obtained radiative broadenings $\hbar\Gamma_{0j}$ with the results from numerical modeling, shown in Fig. 3, shows good agreement. In particular, it is appropriate for the second, third, and fourth states. For the first state, the deviation of the theoretical results from the experimental data is noticeable even at zero magnetic field.

There are several possible reasons for this discrepancy. First, the experimental accuracy of the $\hbar\Gamma_0$ determination is limited by the accuracy of the measurements of the absolute value of the reflectance coefficient, which depends on the quality of the sample surface. It is found to be slightly different for different points on the sample. We estimate this accuracy to be about $\pm 5\%$. Second, for the first exciton state in the wide QW under study, potential fluctuations may vary the spatial exciton coherence volume, thus noticeably varying the radiative decay rate. Measurements at another position on the sample provide a value of $\hbar\Gamma_0$, which deviates by approximately $\pm 5 \mu\text{eV}$ from the presented value, but is still lower than the calculated one.

The theoretically obtained magnetic-field-induced increase of $\hbar\Gamma_0$ reproduces the experimentally obtained behavior for the X2, X3, and X4 exciton states reasonably well. However, it is overestimated by about 15% for the first state. The origin of this effect is unclear. One possible reason may be a small change of the Luttinger parameters γ_1 and γ_2 in the (In,Ga)As QW compared to those for GaAs. This change is not taken into account in our calculations.

The theoretical dependencies of $\hbar\Gamma_0$ on magnetic field for all exciton transitions shown in Fig. 3 are very similar. They are quadratic at small magnetic fields and become linear at large B . The dependencies can be well fitted by the phenomenological formula:

$$\hbar\Gamma_0(B) = \hbar\Gamma_0(0) \left[1 + \alpha \frac{B^2}{B + B_D} \right]. \quad (11)$$

Here $\hbar\Gamma_0(0)$ is the radiative broadening at zero magnetic field, the parameter α describes the slope of the linear dependence at large magnetic field, and parameter B_D is the critical magnetic field when the dependence changes from quadratic to linear. The fitting curves are shown in Fig. 3. The obtained fitting parameters are given in Table I. The parameter $B_D = 2 \text{ T}$ is fixed for all exciton transitions.

This fitting implies that at the magnetic field B_D the exciton behavior deviates from that proposed in the framework of the hydrogenlike model. Earlier, this kind of critical field was used in relation to the exciton transition energy [2]. In particular, the diamagnetic shift exhibits parabolic-to-linear transition at some critical field [6]. Here we observe a similar effect in the behavior of the exciton-light coupling. The critical field B_D is approximately twice smaller than that proposed by the Loudon criterion, $B_L = 4 \text{ T}$ [2]. We note that the analysis

TABLE I. Radiative broadening $\hbar\Gamma_0$ at zero magnetic field and the slope α obtained from the fits of the theoretical and experimental data shown in Fig. 3 by Eq. (11) for the QW under study with $L = 95 \text{ nm}$. Parameter $B_D = 2 \text{ T}$.

State no.	X1	X2	X3	X4
$\hbar\Gamma_0$ (μeV , experiment)	44.8	21.2	6.2	12.0
$\hbar\Gamma_0$ (μeV , theory)	58.2	20.6	5.6	10.0
α (T^{-1} , experiment)	0.19	0.23	0.24	0.15
α (T^{-1} , theory)	0.24	0.24	0.19	0.23

of the diamagnetic shift in Ref. [6] also gives a considerably smaller critical magnetic field of about 1.5 T.

To illustrate the general behavior of the exciton-light coupling in QWs of various widths in magnetic field, we fitted the data presented in Fig. 4 with expression (11) and extracted the parameters B_D and α . The results for states X1 and X2 are shown in Fig. 6. For the X1 state, the critical magnetic field B_D is found to decrease with the QW width rise. The relatively large value of B_D for narrow QWs is naturally explained by the squeezing of the exciton wave function in the QW layer plane caused by the stronger electron-hole Coulomb attraction [34]. The critical field B_D for the X2 state appears to be independent on the QW width within the calculation errors.

The slope α increases for states X1 and X2 and tends to value $\approx 0.25 \text{ T}^{-1}$. A linear interpolation of the calculated dependencies $G_0(B)$ in the range $B = 4\text{--}6 \text{ T}$ for wide QWs ($L \geq 80 \text{ nm}$) gives rise to a slightly larger slope, $\alpha_\infty \approx 0.28 \text{ T}^{-1}$, which can be used for extrapolation of the dependence $\hbar\Gamma_0(B)$ to larger magnetic fields. In particular, the strength of exciton-light coupling can increase about four times in a magnetic field with $B = 10 \text{ T}$, easily achievable in laboratory conditions. Taking into account the average value of $\hbar\Gamma_0(0) = 63 \pm 3 \mu\text{eV}$ for state X1 in wide QWs, we obtain $\hbar\Gamma_0(B) = 240 \mu\text{eV}$ for $B = 10 \text{ T}$. This radiative broadening

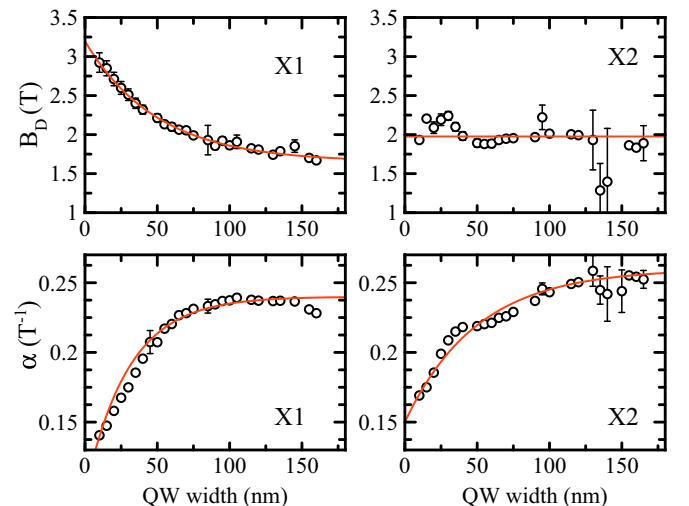


FIG. 6. Parameters B_D and α for the first two quantum-confined exciton states extracted from the calculations presented in Fig. 4 by fitting with expression (11).

may be considerably larger than the nonradiative one in MBE grown heterostructures.

Strong exciton-light coupling attracts considerable attention due to both interesting fundamental questions and possible practical applications. Several possible ways to increase the exciton-light coupling have been discussed in the literature. One of them is the fabrication of so-called Bragg structures with multiple QWs positioned at half wavelength distance from each other. The exciton-light coupling constant in such structures is the sum of the constants of the individual QWs and may be orders of magnitude larger than that of a single QW [1]. This attractive idea meets, however, certain difficulties in the experimental realization [46–48]. Namely, an unavoidable instability of the growth process, in particular when several tens of QWs are grown [47,48], gives rise to an inhomogeneous broadening of the exciton ensemble and, correspondingly, to a strong reduction of the coupling compared to the theoretical predictions. The combination of the two methods, the growth of the Bragg structures and the application of an external magnetic field, is possibly the way to strongly increase the exciton-light coupling in GaAs-based structures.

Another way is to place a QW in a microcavity where the renormalization of photon states may strongly increase the exciton-light coupling [13]. In this case, however, the system is highly sensitive to the geometry of experiment and to the excitation power, therefore simple theoretical models, such as the one employed in present study, are no longer applicable. In recent years, new materials, e.g., the two-dimensional crystals with huge exciton oscillator strength, have been extensively studied (see, e.g., papers [49–53] and references therein). The quality of these crystals is still somewhat limited, therefore the quantitative study of exciton-light coupling is problematic.

V. CONCLUSION

We have experimentally determined the radiative decay rates for the ground and excited quantum-confined exciton states in a wide QW as a function of magnetic field. The radiative decay rates are found to monotonically increase with the magnetic field. This effect is traced to the exciton squeezing by the magnetic-field-induced parabolic potential in the QW plane. We have also calculated the radiative decay rates for the studied QW. In this case we accounted for the In segregation during the QW growth to simulate the real QW potential in the heterostructure under study. The numerically obtained values of $\hbar\Gamma_{0j}$ are in good agreement with those obtained in the experiment for the second, third, and fourth quantum-confined exciton states. For the lowest state, the theory and the experiment significantly deviate ($>10\%$). We suggest this deviation to be due to variations of the exciton in-plane coherence length due to QW potential fluctuations.

We have also modelled the radiative decay rates as a function of the magnetic field and of the QW width for the first four exciton states in (In,Ga)As QWs with 2% indium content. In such QWs, the confinement is “weak” in a sense that the exciton is not squeezed by the QW potential in narrow QWs and easily penetrates into the barrier layers due to their relatively small height. Correspondingly, the radiative decay rate for the ground exciton state has no maximum in such QWs [34]. In such weak QWs, the radiative decay rate is controlled mainly by the overlap of the exciton wave function with the light wave as expressed by the integral in Eq. (3).

The character of the $\Gamma_0(B)$ dependencies has also been investigated. It was found that the radiative decay rate has a quadratic dependence in relatively small magnetic fields, which tends to a linear dependence as the magnetic field rises. The slope of the dependencies was found to be similar for the different quantum-confined exciton states in wide QWs ($L \geq 100$ nm). For narrower QWs, the slope deviates from a constant value which indicates that the quantum confinement notably affects the diamagnetic behavior of the exciton states. This is also seen in the numerical calculations of the exciton wave functions in QWs for which the QW width is comparable to the exciton Bohr diameter (30 nm in GaAs).

In our study we have limited ourselves to (In,Ga)As/GaAs QWs as compared to conventional GaAs/AlGaAs heterostructures. First, we were able to illustrate the role of overlap of the exciton wave function with the light wave, because the confinement in the (In,Ga)As QWs is weak. Second, due to the lattice constant mismatch in the (In,Ga)As/GaAs heterostructures, the degeneracy of the valence band is lifted which allows one to simplify the calculations considering a single heavy-hole valence band only. As a result, we were able to calculate the radiative decay rate for several quantum-confined exciton states and found good agreement with the values obtained by reflectance spectroscopy. The dependence of the radiative decay rate on the magnetic field could be also predicted.

ACKNOWLEDGMENTS

The authors thank I. Ya. Gerlovin and D. R. Yakovlev for fruitful discussions. The financial support of the Russian Foundation for Basic Research (Grant No. 15-52-12019) and the Deutsche Forschungsgemeinschaft in the framework of ICRC TRR 160 is acknowledged. The studied heterostructure was grown in the resource center “Nanophotonics” of St. Petersburg State University. I. V. I. thanks the Russian Foundation for Basic Research for financial support in the framework of Grant No. 16-02-00245 a.

-
- [1] E. L. Ivchenko, *Optical Spectroscopy of Semiconductor Nanostructures* (Springer-Verlag, Berlin-Heidelberg, 2004).
 [2] R. P. Seisyan, Diamagnetic excitons and exciton magnetopolaritons in semiconductors, *Semicond. Sci. Technol.* **27**, 053001 (2012).

- [3] I. A. Yugova, A. Greilich, D. R. Yakovlev, A. A. Kiselev, M. Bayer, V. V. Petrov, Yu. K. Dolgikh, D. Reuter, and A. D. Wieck, Universal behavior of the electron g factor in GaAs/Al_xGa_{1-x}As quantum wells, *Phys. Rev. B* **75**, 245302 (2007).

- [4] M. V. Durnev, M. M. Glazov, and E. L. Ivchenko, Spin-orbit splitting of valence subbands in semiconductor nanostructures, *Phys. Rev. B* **89**, 075430 (2014).
- [5] P. S. Grigoryev, O. A. Yugov, S. A. Eliseev, Yu. P. Efimov, V. A. Lovtcius, V. V. Petrov, V. F. Sapega, and I. V. Ignatiev, Inversion of Zeeman splitting of exciton states in InGaAs quantum wells, *Phys. Rev. B* **93**, 205425 (2016).
- [6] S. Yu. Bodnar, P. S. Grigoryev, D. K. Loginov, V. G. Davydov, Yu. P. Efimov, S. A. Eliseev, V. A. Lovtcius, E. V. Ubyivovk, V. Yu. Mikhailovskii, and I. V. Ignatiev, Exciton mass increase in a GaAs/AlGaAs quantum well in a transverse magnetic field, *Phys. Rev. B* **95**, 195311 (2017).
- [7] J. D. Berger, O. Lyngnes, H. M. Gibbs, G. Khitrova, T. R. Nelson, E. K. Lindmark, A. V. Kavokin, M. A. Kaliteevski, and V. V. Zapasskii, Magnetic-field enhancement of the exciton-polariton splitting in a semiconductor quantum-well microcavity: The strong coupling threshold, *Phys. Rev. B* **54**, 1975 (1996).
- [8] J. Fischer, S. Brodbeck, A. V. Chernenko, I. Lederer, A. Rahimi-Iman, M. Amthor, V. D. Kulakovskii, L. Worschech, M. Kamp, M. Durnev, C. Schneider, A. V. Kavokin, and S. Hofling, Anomalies of a Nonequilibrium Spinor Polariton Condensate in a Magnetic Field, *Phys. Rev. Lett.* **112**, 093902 (2014).
- [9] C. Sturm, D. Solnyshkov, O. Krebs, A. Lemaitre, I. Sagnes, E. Galopin, A. Amo, G. Malpuech, and J. Bloch, Nonequilibrium polariton condensate in a magnetic field, *Phys. Rev. B* **91**, 155130 (2015).
- [10] P. Stepnicki, B. Pietka, F. Morier-Genoud, B. Deveaud, and M. Matuszewski, Analytical method for determining quantum well exciton properties in a magnetic field, *Phys. Rev. B* **91**, 195302 (2015).
- [11] V. P. Kochereshko, M. V. Durnev, L. Besombes, H. Mariette, V. F. Sapega, A. Askitopoulos, I. G. Savenko, T. C. H. Liew, I. A. Shelykh, A. V. Platonov, S. I. Tsintzos, Z. Hatzopoulos, P. G. Savvidis, V. K. Kalevich, M. M. Afanasiev, V. A. Lukoshkin, C. Schneider, M. Amthor, C. Metzger, M. Kamp, S. Hoefling, P. Lagoudakis, and A. Kavokin, Lasing in Bose-Fermi mixtures, *Sci. Rep.* **6**, 20091 (2016).
- [12] J. Wilkes and E. A. Muljarov, Dipolar polaritons in microcavity-embedded coupled quantum wells in electric and magnetic fields, *Phys. Rev. B* **94**, 125310 (2016).
- [13] A. V. Kavokin, J. J. Baumberg, G. Malpuech, and F. P. Laussy, *Microcavities*, 2nd ed. (Oxford University Press, New York, 2017).
- [14] K. Kowalik-Seidl, X. P. Vogle, F. Seilmeier, D. Schuh, W. Wegscheider, A. W. Holleitner, and J. P. Kotthaus, Forming and confining of dipolar excitons by quantizing magnetic fields, *Phys. Rev. B* **83**, 081307(R) (2011).
- [15] Y. Mazuz-Harpaz, K. Cohen, B. Laikhtman, and R. Rapaport, Radiative lifetimes of dipolar excitons in double quantum wells, *Phys. Rev. B* **95**, 155302 (2017).
- [16] Yu. E. Lozovik, I. V. Ovchinnikov, S. Yu. Volkov, L. V. Butov, and D. S. Chemla, Quasi-two-dimensional excitons in finite magnetic fields, *Phys. Rev. B* **65**, 235304 (2002).
- [17] J. Wilkes and E. A. Muljarov, Exciton effective mass enhancement in coupled quantum wells in electric and magnetic fields, *New J. Phys.* **18**, 023032 (2016).
- [18] Y. Y. Kuznetsova, C. J. Dorow, E. V. Calman, L. V. Butov, J. Wilkes, E. A. Muljarov, K. L. Campman, and A. C. Gossard, Transport of indirect excitons in high magnetic fields, *Phys. Rev. B* **95**, 125304 (2017).
- [19] I. Ya. Gerlovina, Yu. K. Dolgikh, S. A. Eliseev, V. V. Ovsyankin, Yu. P. Efimov, V. V. Petrov, I. Vi. Ignatiev, I. E. Kozin, and Y. Masumoto, Fine structure and spin dynamics of excitons in the GaAs/Al_xGa_{1-x}As superlattices, *Phys. Rev. B* **65**, 035317 (2001).
- [20] I. Ya. Gerlovina, Yu. K. Dolgikh, S. A. Eliseev, V. V. Ovsyankin, Yu. P. Efimov, I. V. Ignatiev, V. V. Petrov, S. Yu. Verbin, and Y. Masumoto, Spin dynamics of carriers in the GaAs quantum wells in an external electric field, *Phys. Rev. B* **69**, 035329 (2004).
- [21] I. Ya. Gerlovina, Yu. P. Efimov, Yu. K. Dolgikh, S. A. Eliseev, V. V. Ovsyankin, V. V. Petrov, R. V. Cherbunin, I. V. Ignatiev, I. A. Yugova, L. V. Fokina, A. Greilich, D. R. Yakovlev, and M. Bayer, Electron-spin dephasing in GaAs/AlGaAs quantum wells with a gate-controlled electron density, *Phys. Rev. B* **75**, 115330 (2007).
- [22] I. A. Yugova, A. A. Sokolova, D. R. Yakovlev, A. Greilich, D. Reuter, A. D. Wieck, and M. Bayer, Long Term Hole Spin Memory in the Resonantly Amplified Spin Coherence of InGaAs/GaAs Quantum Well Electrons, *Phys. Rev. Lett.* **102**, 167402 (2009).
- [23] L. Langer, S. V. Poltavtsev, I. A. Yugova, D. R. Yakovlev, G. Karczewski, T. Wojtowicz, J. Kossut, I. A. Akimov, and M. Bayer, Magnetic Field Control of Photon Echo in the Electron-Trion System of a CdTe Quantum Well: Shuffling of Coherences Between Optically Accessible and Inaccessible States, *Phys. Rev. Lett.* **109**, 157403 (2012).
- [24] E. A. Zhukov, O. A. Yugov, I. A. Yugova, D. R. Yakovlev, G. Karczewski, T. Wojtowicz, J. Kossut, and M. Bayer, Resonant spin amplification of resident electrons in CdTe/(Cd, Mg)Te quantum wells subject to tilted magnetic fields, *Phys. Rev. B* **86**, 245314 (2012).
- [25] L. Langer, S. V. Poltavtsev, I. A. Yugova, M. Salewski, D. R. Yakovlev, G. Karczewski, T. Wojtowicz, I. A. Akimov, and M. Bayer, Photon echoes retrieved from semiconductor spins: access to long-term optical memories, *Nat. Photon.* **8**, 851 (2014).
- [26] T. Kazimierzczuk, D. Fröhlich, S. Scheel, H. Stolz, and M. Bayer, Giant Rydberg excitons in the copper oxide Cu₂O, *Nature (London)* **514**, 343 (2014).
- [27] F. Schweiner, J. Main, G. Wunner, M. Freitag, J. Heckötter, C. Uihlein, M. Assmann, D. Fröhlich, and M. Bayer, Magnetoexcitons in cuprous oxide, *Phys. Rev. B* **95**, 035202 (2017).
- [28] Y. Iimura, Y. Segawa, G. E. W. Bauer, M. M. Lin, Y. Aoyagi, and S. Namba, Exciton mixing in a wide GaAs/AlAs quantum well in weak and intermediate magnetic fields, *Phys. Rev. B* **42**, 1478 (1990).
- [29] E. L. Ivchenko, A. V. Kavokin, V. P. Kochereshko, G. R. Posina, I. N. Uraltsev, D. R. Yakovlev, R. N. Bicknell-Tassius, A. Waag, and G. Landwehr, Exciton oscillator strength in magnetic-field-induced spin superlattices CdTe/(Cd, Mn)Te, *Phys. Rev. B* **46**, 7713 (1992).
- [30] M. Sugawara, N. Okazaki, T. Fujii, and S. Yamazaki, Diamagnetic shift and oscillator strength of two-dimensional excitons under a magnetic field in In_{0.53}Ga_{0.47}As/InP quantum wells, *Phys. Rev. B* **48**, 8848 (1993).
- [31] A. V. Kavokin, A. I. Nesvizhskii, and R. P. Seisyan, Exciton in semiconductor quantum well in strong magnetic field, *Semiconductors* **27**, 530 (1993) [*Fiz. Tekh. Poluprovodn.* **27**, 977 (1993)].

- [32] I. Aksenov, Y. Aoyagi, J. Kusano, T. Sugano, T. Yasuda, and Y. Segawa, Temporal dynamics of a magnetoexciton in a quantum well, *Phys. Rev. B* **52**, 17430 (1995).
- [33] B. S. Monozon and P. Schmelcher, Optical absorption by excitons in semiconductor quantum wells in tilted magnetic and electric fields, *Phys. Rev. B* **82**, 205313 (2010).
- [34] E. S. Khramtsov, P. A. Belov, P. S. Grigoryev, I. V. Ignatiev, S. Yu. Verbin, Yu. P. Efimov, S. A. Eliseev, V. A. Lovtcius, V. V. Petrov, and S. L. Yakovlev, Radiative decay rate of excitons in square quantum wells: Microscopic modeling and experiment, *J. Appl. Phys.* **119**, 184301 (2016).
- [35] R. J. Elliott and R. Loudon, Theory of fine structure on the absorption edge in semiconductors, *J. Phys. Chem. Solids* **8**, 382 (1959).
- [36] R. C. Iotti and L. C. Andreani, Crossover from strong to weak confinement for excitons in shallow or narrow quantum wells, *Phys. Rev. B* **56**, 3922 (1997).
- [37] A. D'Andrea, N. Tomassini, L. Ferrari, M. Righini, S. Selci, M. R. Bruni, D. Schiumarini, and M. G. Simeone, Optical properties of stepped $\text{In}_x\text{Ga}_{1-x}\text{As}/\text{GaAs}$ quantum wells, *J. Appl. Phys.* **83**, 7920 (1998).
- [38] B. Gerlach, J. Wüsthoff, M. O. Dzero, and M. A. Smondyrev, Exciton binding energy in a quantum well, *Phys. Rev. B* **58**, 10568 (1998).
- [39] D. Schiumarini, N. Tomassini, L. Piloizzi, and A. D'Andrea, Polariton propagation in weak-confinement quantum wells, *Phys. Rev. B* **85**, 045207 (2012).
- [40] K. Sivalertporn, L. Mouchliadis, A. L. Ivanov, R. Philp, and E. A. Muljarov, Direct and indirect excitons in semiconductor coupled quantum wells in an applied electric field, *Phys. Rev. B* **82**, 075303 (2010).
- [41] A. V. Trifonov, S. N. Korotan, A. S. Kurdyubov, I. Ya. Gerlovin, I. V. Ignatiev, Yu. P. Efimov, S. A. Eliseev, V. V. Petrov, Yu. K. Dolgikh, V. V. Ovsyankin, and A. V. Kavokin, Nontrivial relaxation dynamics of excitons in high-quality InGaAs/GaAs quantum wells, *Phys. Rev. B* **91**, 115307 (2015).
- [42] P. S. Grigoryev, A. S. Kurdyubov, M. S. Kuznetsova, I. V. Ignatiev, Yu. P. Efimov, S. A. Eliseev, V. V. Petrov, V. A. Lovtcius, and P. Yu. Shapochkin, Excitons in asymmetric quantum wells, *Superlattices Microstruct.* **97**, 452 (2016).
- [43] M. M. Voronov, E. L. Ivchenko, V. A. Kosobukin, and A. N. Poddubnyi, Specific features in reflectance and absorbance spectra of one-dimensional resonant photonic crystals, *Phys. Solid State* **49**, 1792 (2007) [*Fiz. Tverd. Tela* **49**, 1709 (2007)].
- [44] J. M. Luttinger, Quantum Theory of Cyclotron Resonance in Semiconductors: General Theory, *Phys. Rev.* **102**, 1030 (1956).
- [45] I. Vurgaftman, J. R. Meyer, and L. R. Ram-Mohan, Band parameters for III-V compound semiconductors and their alloys, *J. Appl. Phys.* **89**, 5815 (2001).
- [46] S. V. Poltavtsev, Yu. P. Efimov, Yu. K. Dolgikh, S. A. Eliseev, V. V. Petrov, and V. V. Ovsyankin, Extremely low inhomogeneous broadening of exciton lines in shallow (In, Ga)As/GaAs quantum wells, *Solid State Commun.* **199**, 47 (2014).
- [47] Y. Chen, N. Maharjan, Z. Liu, M. L. Nakarmi, V. V. Chaldyshev, E. V. Kundelev, A. N. Poddubny, A. P. Vasilev, M. A. Yagovkina, and N. M. Shakyia, Resonant optical properties of AlGaAs/GaAs multiple-quantum-well based Bragg structure at the second quantum state, *J. Appl. Phys.* **121**, 103101 (2017).
- [48] A. S. Bolshakov, V. V. Chaldyshev, E. E. Zavarin, A. V. Sakharov, W. V. Lundin, A. F. Tsatsulnikov, and M. A. Yagovkina, Room temperature exciton-polariton resonant reflection and suppressed absorption in periodic systems of InGaAs quantum wells, *J. Appl. Phys.* **121**, 133101 (2017).
- [49] M. M. Glazov, E. L. Ivchenko, G. Wang, T. Amand, X. Marie, B. Urbaszek, and B. L. Liu, Spin and valley dynamics of excitons in transition metal dichalcogenide monolayers, *Phys. Status Solidi B* **252**, 2349 (2015).
- [50] M. Selig, G. Berghäuser, A. Raja, P. Nagler, C. Schüller, T. F. Heinz, T. Korn, A. Chernikov, E. Malic, and A. Knorr, Excitonic linewidth and coherence lifetime in monolayer transition metal dichalcogenides, *Nat. Commun.* **7**, 13279 (2016).
- [51] T. Godde, D. Schmidt, J. Schmutzler, M. Assmann, J. Debus, F. Withers, E. M. Alexeev, O. Del Pozo-Zamudio, O. V. Skrypka, K. S. Novoselov, M. Bayer, and A. I. Tartakovskii, Exciton and trion dynamics in atomically thin MoSe_2 and WSe_2 : Effect of localization, *Phys. Rev. B* **94**, 165301 (2016).
- [52] X. Li, L. Tao, Z. Chen, H. Fang, X. Li, X. Wang, J.-B. Xu, and H. Zhu, Graphene and related two-dimensional materials: Structure-property relationships for electronics and optoelectronics, *Appl. Phys. Rev.* **4**, 021306 (2017).
- [53] S. Dufferwiel, S. Schwarz, F. Withers, A. A. P. Trichet, F. Li, M. Sich, O. Del Pozo-Zamudio, C. Clark, A. Nalitov, D. D. Solnyshkov, G. Malpuech, K. S. Novoselov, J. M. Smith, M. S. Skolnick, D. N. Krizhanovskii, and A. I. Tartakovskii, Exciton-polaritons in van der Waals heterostructures embedded in tunable microcavities, *Nat. Commun.* **6**, 8579 (2015).